Acta Cryst. (1998). A**54**, 191–198

Primary Extinction and Absorption: a Theoretical Approach Based on the Takagi–Taupin Equations. Application to Spherical Crystals

F. N. CHUKHOVSKII,† A. HUPE, E. ROSSMANITH* AND H. SCHMIDT

Mineralogisch-Petrographisches Institut der Universität Hamburg, D-20146 Hamburg, Grindelallee 48, Germany. E-mail: rossmanith@mineralogie.uni-hamburg.de

(*Received 28 June 1997; accepted 23 September 1997*)

Abstract

The primary-extinction problem for X-ray diffraction by perfect crystals is treated using the Becker–Coppens iterative procedure within the Takagi–Taupin equations. An analytical approximation for the primary-extinction factor y_p describing both the effects of the X-ray multiple scattering and the absorption processes within the perfect crystal of an arbitrary shape is derived. The solution differs from the known expressions given by Zachariasen and Becker & Coppens on the basis of the Hamilton–Darwin intensity transfer equations and in the limiting case of a non-absorbing crystal it concurs with the Kato–Becker formula found in the Laue approximation of the dynamical theory. The theoretical results are consistent with experimental data of a number of reflections of Ge and Si single-crystal spheres measured at X-ray wavelengths λ = 0.56, 0.71 and 1.54 Å with a laboratory CAD-4 and a Huber four-circle diffractometer at HASYLAB, DESY, Hamburg, Germany. Two novel features are discussed. First, it is shown that by neglecting the X-ray absorption effect the calculated extinction factor y_p is close to the value given by the Becker–Coppens formula. Second, it was found that for absorbing spherical crystals with $\mu R \geq 1$ absorption effects cannot be treated separately from the primary-extinction phenomenon because of imaginary dispersion corrections to the atomic form factors. The experimental data are fitted to the Becker–Coppens and present theoretical models. The best fits are found to relate to the present model and produce relatively low R factors of 3 to 6% for the Bragg intensities measured in the cases of Si and Ge spherical crystals.

1. Introduction

The problem of primary extinction and absorption (PEXA) of finite diffracting perfect crystals has attracted a great deal of debate in X-ray and thermal-neutron diffraction physics as to whether a significant improvement of the purely kinematical approach is possible for crystals of an arbitrary shape.

As is well known, primary extinction is caused by the coherent scattering of X rays in a single-crystalline block in contrast to secondary extinction, which is due to incoherent scattering in a mosaic crystal. Despite the great physical difference, these phenomena are first treated with a theoretical approach based on the Hamilton–Darwin transfer equations (Hamilton, 1957), although the necessity for evaluating the primary-extinction factor using the X-ray dynamical theory (see *e.g.* Laue, 1960) was very clear to authors of the pioneering papers (Zachariasen, 1967; Becker & Coppens, 1974, B&C hereinafter; Werner, 1974). Later, there were several papers (Kato, 1976; Becker, 1977; Olekhnovich & Olekhnovich, 1978; Becker & Dunstetter, 1984; Werner *et al.*, 1986; Al Haddad & Becker, 1990, H&B hereinafter), in which the general approach to evaluate the primary-extinction factor by use of the dynamical Takagi–Taupin equations (Takagi, 1962, 1969; Taupin, 1964, 1967) was discussed. A meaningful primary-extinction solution (except for X-ray absorption) was first found by Kato (1976) and Becker (1977) and corresponds to the Laue approximation of the point-source diffractive function that describes X-ray diffraction by finite convex-shaped crystals. On the other hand, the most advanced H&B calculations performed for the case of spherical crystals ignore the X-ray absorption effects and therefore are irrelevant for dealing directly with measured data for absorbing crystals.

In this work, we propose a quantitative model of the PEXA based on the B&C iterative procedure for solving the dynamical Takagi–Taupin equations (TTE). We follow closely the ideas laid out by B&C. B&C's paper forms the basis of the present approach to solve the TTE, taking into account the effect of both X-ray multiple scattering and absorption within a finite single crystal, although many of the aspects of the PEXA phenomenon considered here are significantly different from the Hamilton–Darwin transfer equations. It is remarkable that as the coherent scattering and absorption are considered the B&C procedure can still be applied. Since a thorough theoretical investigation of the point-source diffractive function for an arbitrary convex-shaped

† Permanent address: Institute of Crystallography, Russian Academy of Sciences, Moscow 117333, Leninsky Prospect, 59, Russia. Supported under DFG grant No. 436 RUS 17/6/96.

ISSN 0108-7673

absorbing crystal is inaccessible at the present time, we pursue our analysis of the primary-extinction problem with the Laue approximation including the X-ray absorption effects explicitly.

In the following, we briefly give a general treatment of the PEXA problem based on the dynamical TTE. Then, the solution will be applied to the most important case of spherical crystals. Finally, we compare the results from the present study with those of B&C as well as with Bragg intensity measurements of Si and Ge single crystals performed with a Cu X-ray tube in the laboratory CAD-4 diffractometer and the Huber four-circle diffractometer at HASYLAB, DESY.

2. General foundation of the primary-extinction and absorption problem

The TTE linking the plane-wave amplitudes E_0 and E_h of the transmitted and diffracted wave fields can be written as (Takagi, 1969)

$$\begin{aligned} \partial E_0/\partial s_0 - i(\chi_0/2)KE_0 &= i(\chi_{-h}/2)KCE_h \\ \partial E_h/\partial s_h - i[(\chi_0 - \alpha)/2]KE_h &= i(\chi_h/2)KCE_0. \end{aligned} \tag{1}$$

The system of the dynamical equations (1) is written for a section of a convex-shaped crystal parallel to the diffraction plane. An oblique coordinate system is defined with axes parallel to the incident- and diffracted-wave directions (coordinates s_0 and s_h). χ_0 and χ_h are the complex zero and h Fourier components of the dielectric susceptibility function of a crystal, C is the polarization factor equal to 1 or $\cos 2\theta$ for σ- or π-polarized X rays, respectively, θ is the Bragg angle related to the diffraction vector $\mathbf{h}$, $K = 2\pi/\lambda$ is the magnitude of the X-ray wavevector $\mathbf{k}$ and λ is the wavelength. The parameter α is given by $\alpha = 2\varepsilon_1 \sin 2\theta$ and the angle ε_1 describes the deviation of the incident X-ray plane wave from the exact Bragg direction in the diffraction plane.

We follow closely the B&C procedure and rewrite (1) in the integral form

$$E_h(s_0, s_h) = i(\chi_h C/2) \int_{u_2^0}^{s_h} \mathrm{d}u_2 \exp\{iK[(\chi_0 - \alpha)/2](s_h - u_2)\} \times E_0(s_0, u_2), \tag{2}$$

$$\begin{aligned} E_0(s_0, s_h) = -i(\chi_{-h}\chi_h C^2/4) &\int_{u_1^0}^{s_0} \mathrm{d}u_1 \\ &\times \int_{u_2^0}^{s_h} \mathrm{d}u_2 \exp\{iK[(\chi_0 - \alpha)/2](s_h - u_2) \\ &+ iK(\chi_0/2)(s_0 - u_1)\} E_0(u_1, u_2) \\ &+ \exp[iK(\chi_0/2)(s_0 - u_1^0)]. \end{aligned} \tag{3}$$

The diffracted power $P(\varepsilon_1)$ for a given ε_1 is defined as (see *e.g.* B&C for details)

$$P(\varepsilon_1) = \iint_{s_0, s_h \in S} |E_h(s_0, s_h)|^2 (\mathbf{s}_h \, \mathrm{d}\mathbf{S}) \tag{4}$$

and $(\mathbf{s}_h \, \mathrm{d}\mathbf{S})$ is the surface element $\mathrm{d}S$ of the orthogonal projection (S) of a crystal parallel to the diffracted radiation direction $\mathbf{s}_h$.

The main principles of the iterative approach to build up the solution of the integral equations (2) and (3) are the same as those in B&C. Under the same conditions assumed by B&C and going through simple but cumbersome calculations, we derive the following expression for the diffracted-wave amplitude scattered to point M in the diffraction plane:

$$\begin{aligned} E_h(M) = i(\chi_h C/2) &\int_{u_2^0}^{u_2(M)} \mathrm{d}u_2(M_1) \\ &\times \exp\{iK[(\chi_0 - \alpha)/2]t_2'(M_1) + iK(\chi_0/2)t_1(M_1)\} \\ &\times J_0\{(\chi_{-h}\chi_h)^{1/2}K|C|[t_1(M_1)t_2'(M_1)]^{1/2}\}, \end{aligned} \tag{5}$$

where $J_0(x)$ is the zero-order Bessel function. In (5), we have introduced the well known path lengths t_1 and t_2' of the incident and diffracted beams.

It is worth noting that (5) corresponds to the Laue approximation of the point-source diffractive function first introduced into the PEXA problem by Becker (1977).

By going from $P(\varepsilon_1)$ by integration of (4) with (5) over ε_1, the integrated intensity $\wp$ of the diffracted radiation, under the condition of unit incident intensity, can be readily obtained:

$$\wp = QVy_p \tag{6}$$

and, under the Laue approximation of the point-source diffractive function, the PEXA factor y_p is determined by

$$\begin{aligned} y_p = V^{-1} &\iiint_V \mathrm{d}V(M) \exp\{-\mu[t_1(M) + t_2'(M)]\} \\ &\times |J_0\{(\chi_{-h}\chi_h)^{1/2}K|C|[t_1(M)t_2'(M)]^{1/2}\}|^2. \end{aligned} \tag{7}$$

In the derivation of (6) and (7), well known formulae have been used:

$$\chi_h = -(r_e\lambda^2/\pi V_c)F_h, \tag{8}$$

$$Q = |r_e F_h C/V_c|^2 \lambda^3/\sin 2\theta, \tag{9}$$

where F_h is the complex structure factor, V_c is the unit-cell volume, and r_e is the classical radius of an electron, $r_e = 2.8 \times 10^{-15}$ m.

The integration in (7) is over the crystal volume V and the linear absorption coefficient μ is equal to

$$\mu = 2(r_e\lambda/V_c)\Im(F_0). \tag{10}$$

By definition, $\Im(F_0) > 0$.

The solutions (4)–(7) are independent of special conventions in the crystal and, hence, they can be applied to calculate the angular distribution [the rocking curve, see (4) and (5)] and the integrated reflectivity [and therefore the PEXA factor as well, see (6) and (7)] for a single crystal of arbitrary convex shape.

The solution of the dynamical equations (1) for the PEXA factor y_p is remarkably different from the corresponding expression by B&C [*cf.* equations (14) and (*B*6) in B&C]. It is interesting that the integrand on the right-hand side of (7) depends on the combination of the path lengths $t_1(M)$ and $t_2'(M)$ as in the B&C formula. The solution (7) for the PEXA factor does not depend on any assumptions (special models) regarding the diffracting cross section $\sigma(\varepsilon_1)$ per unit volume that is basically important in the B&C theory.

Essentially, the analytical expression (7) is rather simple and exactly corresponds to the Laue approximation of the point-source diffractive function, Kato's (1976) and Becker's (1977) formula, additionally taking into consideration the X-ray absorption effects. In the limiting case of first-order X-ray scattering, the Bessel function $J_0(x)$ of the integrand in (5) and (7) should be set to unity and then (7) reduces to the well known absorption-correction formula of the kinematical theory of X-ray diffraction (*cf. e.g.* Maslen, 1992). Neglecting the imaginary part of the anomalous-dispersion correction for the atomic form factor $f, f = f_0 + f' + if''$, *i.e.* in the case of $f'' = 0$, (7) is identical to expression (11) given in H&B.

3. Primary extinction and absorption factor for a spherical crystal

Here we wish to discuss the case of a spherical crystal, for which the solution (7) can be reduced to closed form. Correspondingly, the expression for the PEXA factor y_p is rewritten as

$$y_p = (3/4\pi R^3) \int_0^R \mathrm{d}r\, r^2 \int_{-1}^{1} \mathrm{d}\cos\vartheta \times \int_0^{2\pi} \mathrm{d}\varphi \exp[-\mu(t_1 + t_2')] |J_0[\nu(t_1 t_2')^{1/2}]|^2, \quad (11)$$

where the path lengths t_1 and t_2' are defined by

$$t_1 = [R^2 - r^2\cos^2\vartheta - r^2\sin^2\vartheta\sin^2(\varphi+\theta)]^{1/2} + r\sin\vartheta\cos(\varphi+\theta) \quad (12)$$

$$t_2' = [R^2 - r^2\cos^2\vartheta - r^2\sin^2\vartheta\sin^2(\varphi-\theta)]^{1/2} - r\sin\vartheta\cos(\varphi-\theta) \quad (13)$$

and r, ϑ and φ are the spherical coordinates related to the Cartesian coordinate system (xyz) with the axis z perpendicular to the diffracting plane.

The complex parameter ν introduced in (11) is

$$\nu = 2r_e\lambda|C|/V_c(F_hF_{-h}) \equiv (1/L_{\mathrm{ext}})(1 + i\kappa). \quad (14)$$

L_{ext} is the extinction length and κ/L_{ext} is the dynamical absorption coefficient.

Expressions (11)–(14) together with (10) can be used for calculating the PEXA factors of spherical crystals.

For completeness of this paper, we give a brief resume of the theoretical results for the primary-extinction correction from B&C. The B&C theory yields the following analytical approximation $y_{\mathrm{B\&C}}$ for the primary-extinction correction:

$$y_{\mathrm{B\&C}} = \left(1 + 2x + \{A(\theta)x^2/[1 + B(\theta)x]\}\right)^{-1} \quad (15)$$

with

$$A(\theta) = 0.20 + 0.45\cos 2\theta$$
$$B(\theta) = 0.22 - 0.12(0.5 - \cos 2\theta). \quad (16)$$

Using the notation $X = R/(2L_{\mathrm{ext}})$, the extinction parameter x is defined by

$$x = \tfrac{3}{2}X^2 \quad (17)$$

with $F_h = F_{-h}^*$.

As has been pointed out by H&B, for non-absorbing crystals, expression (15) successfully follows the average slope of the Laue approximation solution [equation (11) in H&B] as a function of the extinction parameter x. This is why we will compare the results of the present study for the PEXA factor with $y_{\mathrm{B\&C}}$ multiplied by the transmission coefficient

$$A = V^{-1} \iiint_V \mathrm{d}V \exp[-\mu(t_1 + t_2')]. \quad (18)$$

4. Comparison of the theoretical models with measurements of spherical Si and Ge single crystals

The Si and Ge crystals used for the experiments were ground to spheres in a sphere mill. The surface roughness caused by the mechanical treatment of the crystal spheres in the sphere mill was removed by etching. In this way, nearly ideal crystal spheres with radius $R_{\mathrm{Si}} = 85$ and $R_{\mathrm{Ge}} = 65$ μm were obtained.

Bragg intensity profiles of various reflections of the cubic Si (unit-cell constant $a = 5.4346$ Å, displacement parameter $B = 0.46$ Å^2) and Ge ($a = 5.6578$ Å, $B = 0.56$ Å^2) were measured at various wavelengths (Si: 1.5418, 0.5608 Å; Ge: 1.5418, 0.7107 Å) in the routine ω step-scanning mode with the Huber four-circle diffractometer at HASYLAB (DESY, Hamburg, Germany) at beamline D3 of the storage ring DORIS III. In both cases, the crystal spheres were also used for Bragg-intensity measurements in a routine ω–2θ scanning mode with an Enraf–Nonius CAD-4 diffractometer in the laboratory using a Cu X-ray tube.

Table 1. *Absorption and extinction correction for Si*

Standard uncertainty of I_{obs} is caused by counting statistics $\sigma < 1\%$.

(*a*) Synchrotron radiation
$\lambda = 0.5608$ Å, $f' = 0.0522$, $f'' = 0.0431$, $\mu = 6.789\ cm^{-1}$. $A_{min} = 0.916$ (111), $A_{max} = 0.918$ (12,12,0); $X_{min} = 0.35$ (12,12,0), $X_{max} = 5.7$ (022)

h	k	l	$\sin\theta/\lambda$ (Å^{-1})	$A^*y_{B\&C}$	y present	I_{calc} (counts s^{-1}) B&C	I_{calc} (counts s^{-1}) present	I_{obs} (counts s^{-1})
1	1	1	0.159	0.070	0.072	145.9	148.8	164.0
0	2	2	0.260	0.060	0.065	104.1	111.1	109.0
0	−2	−2						105.6
0	0	4	0.369	0.074	0.077	64.1	66.2	63.3
3	3	3	0.479	0.136	0.138	31.2	31.4	34.2
−3	−3	−3						32.5
0	4	4	0.521	0.103	0.106	36.6	37.5	39.2
0	−4	−4						37.8
4	4	4	0.638	0.140	0.141	24.8	24.8	26.2
−4	−4	−4						25.2
0	0	8	0.738	0.186	0.186	18.2	10.0	18.7
0	0	−8						19.3
0	6	6	0.782	0.211	0.204	15.8	15.1	17.1
5	5	5	0.798	0.321	0.286	10.9	9.7	10.0
0	8	8	1.043	0.417	0.391	7.2	6.7	6.8
0	0	12	1.106	0.474	0.459	5.9	5.7	5.7
7	7	7	1.117	0.615	0.638	3.6	3.7	3.4
8	8	8	1.277	0.620	0.627	3.5	3.5	3.2
0	0	16	1.475	0.750	0.757	2.1	2.1	1.7
12	12	0	1.564	0.792	0.796	1.7	1.7	1.4
I_0 (counts s^{-1} m^{-2}) × 10^{14}						8.1 (7)	8.1 (7)	
R						0.058	0.054	

(*b*) Synchrotron radiation
$\lambda = 1.5418$ Å, $f' = 0.2541$, $f'' = 0.3302$, $\mu = 143.0\ cm^{-1}$. $A_{min} = 0.19$ (111), $A_{max} = 0.27$ ($\bar{5}33$); $X_{min} = 6.1$ ($\bar{5}33$), $X_{max} = 15.7$ (022)

h	k	l	$\sin\theta/\lambda$ (Å^{-1})	$A^*y_{B\&C}$	y present	I_{calc} (counts s^{-1}) B&C	I_{calc} (counts s^{-1}) present	I_{obs} (counts s^{-1})
1	1	1	0.160	0.005	0.011	43.9	34.3	33.7
0	2	2	0.261	0.005	0.014	36.7	38.5	35.5
1	1	3	0.306	0.008	0.021	22.7	21.4	20.7
0	0	4	0.368	0.007	0.021	28.1	32.3	29.1
1	3	3	0.402	0.011	0.030	19.1	19.5	19.5
2	2	4	0.451	0.009	0.029	26.0	31.0	28.9
1	5	1	0.479	0.015	0.041	18.8	19.5	22.3
3	3	3	0.479	0.015	0.041	18.8	19.5	20.2
0	4	4	0.521	0.013	0.039	28.9	33.1	32.6
3	5	1	0.545	0.021	0.054	22.7	21.8	23.4
0	2	6	0.583	0.024	0.050	51.1	40.5	39.1
−5	3	3	0.604	–	0.068	–	29.5	32.4
I_0 (counts s^{-1} m^{-2}) × 10^{14}						4.0 (6)†	1.5 (1)	
R						0.127†	0.058	

From analyses of the experimental intensity profiles, it could be concluded that the mosaic spread η of the two samples is zero, *i.e.* η, fitted to the data in the manner described by Rossmanith (1993*a*), was of the order of the minimum possible step width (0.001°) of the ω scan. It was assumed that the Si sample as well as the Ge sample used for measurement embraces only one single block (Rossmanith, 1993*b*; Schmidt, 1995). In the case of Ge, however, discrepancies in the integrated intensities of some of the measured Friedel pairs – much larger than three times the standard uncertainty caused by counting statistics ($\sigma \leq 1\%$) – were observed (Table 2*c*), indicating, at least, distortions in particular directions of the crystal.

In Tables 1 and 2, the corrections obtained for the PEXA defined in (15) is compared with the results of the present approach defined in (7). In the heading of each table, the dispersion corrections f' and f'' of the atomic form factor and the corresponding linear absorption coefficient obtained by use of (10) are listed. Also, the

Table 1 (*cont.*)

(*c*) Cu $K\alpha$ tube
$\lambda = 1.5418$ Å, $f' = 0.2541$, $f'' = 0.3302$, $\mu = 143.0\ \text{cm}^{-1}$. $A_{\min} = 0.19$ (111), $A_{\max} = 0.27$ (533); $X_{\min} = 6.1$ (533), $X_{\max} = 15.7$ (220)

h	k	l	$\sin\theta/\lambda$ (Å^{-1})	$A^*y_{B\&C}$	y present	I_{calc} (counts s^{-1}) B&C	I_{calc} (counts s^{-1}) present	I_{obs} (counts s^{-1})
1	1	1	0.160	0.006	0.011	52.8	42.3	44.6
−1	−1	−1						43.9
2	2	0	0.261	0.006	0.015	39.5	40.7	39.5
−2	−2	0						39.0
3	1	1	0.306	0.010	0.023	22.8	21.3	22.0
−3	−1	−1						20.7
4	0	0	0.369	0.009	0.024	24.6	27.4	27.0
−4	0	0						27.5
3	3	1	0.402	0.013	0.033	15.3	15.2	15.5
−3	−3	−1						15.3
4	2	2	0.452	0.010	0.030	16.9	20.8	20.2
−4	−2	−2						19.4
5	1	1	0.479	0.016	0.042	13.0	13.6	13.9
−5	−1	−1						13.6
3	3	3	0.479	0.016	0.042	13.0	13.6	14.1
−3	−3	−3						12.1
4	4	0	0.522	0.016	0.043	24.1	26.7	26.7
−4	−4	0						26.1
5	3	1	0.546	0.026	0.060	20.6	19.3	20.6
−5	−3	−1						19.6
6	2	0	0.583	0.028	0.055	51.8	41.5	41.5
−6	−2	0						42.1
5	3	3	0.605	–	0.073	–	33.1	34.6
−5	−3	−3		–		–		32.1
I_0 (counts s^{-1} m^{-2}) × 10^{14}						5.2 (6)‡	2.1 (1)	
R						0.108‡	0.030	

† Calculated with $n = 11$ reflections. ‡ Calculated with $n = 22$ reflections.

range of the transmission factor A defined by (18) and the range of the ratio X are presented.

Taking into account the polarization properties of the incident and diffracted beams, the PEXA factors given in the tables are calculated using the relation

$$y_p = (Y_\perp P_\perp + y_\parallel P_\parallel)/P, \tag{19}$$

where the polarization factors $P_\perp$, $P_\parallel$ and P are

$$\begin{aligned} P_\perp &= \tfrac{1}{2}(1+Q) \\ P_\parallel &= \tfrac{1}{2}(1-Q)\cos^2 2\theta \\ P &= P_\perp + P_\parallel. \end{aligned} \tag{20}$$

In the case of the synchrotron-radiation experiments, Q is the polarization ratio. In the case of the laboratory CAD-4 experiments, where a perfect-crystal monochromator with Bragg angle θ_M is used, the PEXA factor is readily shown to be determined by

$$y_p = \frac{y_\perp|\cos 2\theta_M| + y_\parallel \cos^2 2\theta}{|\cos 2\theta_M| + \cos^2 2\theta}. \tag{21}$$

Using the observed integrated intensities $I_{obs}(h)$ and the relation

$$I_0(h) = I_{obs}(h)/Q(h)Vy_p(h) \tag{22}$$

for each extinction model and each reflection, an individual scale factor $I_0(h)$ was calculated. The mean values $\bar{I}_0$ of $I_0(h)$ for the three PEXA models, given at the bottom of the tables, were then used for the determination of the corresponding calculated integrated intensity

$$I_{calc}(h) = \bar{I}_0 Q(h) V y_p(h). \tag{23}$$

For particular combinations of the extinction parameter x and the Bragg angle θ, complex results are obtained for the B&C PEXA correction. In such cases, the corresponding mean scale factor $\bar{I}_0$(B&C) was calculated with the reduced number of reflections.

The residuals R listed in the last line of each table are calculated according to

$$R = \sum |I_{obs}(h) - I_{calc}| \Big/ \sum I_{obs}(h). \tag{24}$$

In Tables 1(*a*), (*b*) and (*c*), the results of the comparison for Si are presented. Table 1(*a*) shows an example of negligible absorption with a nearly constant transmission coefficient A. A fairly good agreement between $A^*y_{B\&C}$ and the present PEXA, y_p, is found in this case, where the greatest $|y_p - y_{B\&C}|/y_p$ is 12% for the 555 reflection. Tables 1(*b*) and (*c*) differ in the polarization factors used. In this case of intermediate absorption, the present PEXA

Table 2. *Absorption and extinction correction for Ge*

Standard deviation of I_{obs} caused by counting statistics $\sigma < 1\%$

(*a*) Synchrotron radiation
$\lambda = 0.7107$ Å, $f' = 0.1547, f'' = 1.8001$, $\mu = 318.7$ cm^{-1}. $A_{min} = 0.07$ (111), $A_{max} = 0.15$ (0,10,10); $X_{min} = 1.38$ (13,3,1), $X_{max} = 13.5$ (220)

h	k	l	$\sin\theta/\lambda$ (Å^{-1})	$A^*y_{B\&C}$	y present	I_{calc} (counts s^{-1}) B&C	I_{calc} (counts s^{-1}) present	I_{obs} (counts s^{-1})
1	1	1	0.153	0.002	0.007	132.0	120.6	126.9
2	2	0	0.250	0.002	0.009	102.9	146.1	139.6
3	1	1	0.293	0.003	0.010	60.1	59.3	61.6
4	0	0	0.354	0.003	0.011	66.3	93.0	94.0
3	3	3	0.459	0.005	0.016	33.2	34.6	38.0
4	4	4	0.612	0.006	0.023	30.7	39.7	41.5
8	0	0	0.707	0.008	0.031	24.9	30.5	30.5
8	4	0	0.791	0.010	0.039	21.3	24.6	25.1
8	8	0	1.000	0.021	0.066	16.6	15.9	16.2
7	7	7	1.072	0.039	0.090	11.6	8.3	8.3
12	4	0	1.118	0.032	0.085	16.4	13.5	13.4
13	3	1	1.183	0.055	0.111	11.7	7.3	6.8
8	8	8	1.225	0.047	0.106	18.0	12.6	11.6
0	10	10	1.250	0.051	0.111	18.8	12.6	11.6
I_0 (counts s^{-1} m^{-2}) $\times 10^{14}$						55 (16)	17 (1)	
R						0.194	0.039	

(*b*) Synchrotron radiation
$\lambda = 1.5410$ Å, $f' = -1.0885, f'' = 0.885$, $\mu = 339.2$ cm^{-1}. $A_{min} = 0.06$ (111), $A_{max} = 0.15$ (4$\bar{4}$4); $X_{min} = 9.6$ (53$\bar{3}$), $X_{max} = 27.1$ (220)

h	k	l	$\sin\theta/\lambda$ (Å^{-1})	$A^*y_{B\&C}$	y present	I_{calc} (counts s^{-1}) B&C	I_{calc} (counts s^{-1}) present	I_{obs} (counts s^{-1})
1	1	1	0.153	0.001	0.004	115.7	88.8	86.4
2	2	0	0.250	0.001	0.006	109.0	129.7	129.4
3	1	1	0.293	0.002	0.009	69.8	66.0	65.7
4	0	0	0.353	0.002	0.011	90.2	109.9	97.8
3	3	1	0.385	0.003	0.014	62.2	62.0	60.3
4	2	2	0.433	0.003	0.015	86.9	104.3	105.3
5	1	1	0.459	0.004	0.021	62.3	61.9	65.3
3	3	3	0.459	0.004	0.021	62.3	62.0	65.8
4	4	0	0.500	0.004	0.021	95.0	107.5	108.0
5	3	−1	0.523	0.006	0.028	72.5	67.1	71.1
6	2	0	0.559	0.006	0.028	128.9	122.5	121.5
5	3	−3	0.579	0.011	0.037	122.6	81.4	85.4
4	−4	4	0.612	–	0.036	–	173.8	163.3
I_0 (counts s^{-1} m^{-2}) $\times 10^{14}$						24 (4)†	4.7 (2)	
R						0.139†	0.037	

factor is about two to three times larger than that of the B&C model resulting in a smaller scale factor I_0. $y_{B\&C}$ for the 533 reflections becomes complex and therefore is not included in Tables 1(*b*) and (*c*).

Tables 2(*a*), (*b*) and (*c*) demonstrate the case of high absorption. As for intermediate absorption, the present PEXA factor is larger than that of the B&C model (see also Fig. 2), again resulting in smaller scale factors. In the case of the CAD-4 experiments (Tables 1*c* and 2*c*), nearly equivalent scale factors are obtained with the present PEXA factor. The magnitude of this scale factor agrees well with the incident intensity estimated experimentally to be about 1 to 2 $\times 10^{14}$ counts s^{-1} m^{-2}. The B&C scale factor, on the other hand, results in different values for Ge and Si and does not provide the experimentally estimated magnitude of the incident beam.

Qualitively, the agreement between the behavior of the two PEXA factors, which is dictated by the ratio X, is apparent (see Figs. 1 and 2). However, as pointed out above, some significant quantitative differences exist between the values of y_p and $y_{B\&C}$ in the case of high X-ray absorption (Fig. 2).

Comparison of the calculated and observed intensities and the residuals R clearly shows that the present model for absorption and extinction results in improved agreement between theory and experiment not only for the case of high absorption (Tables 2*a*, *b*, *c*) but for intermediate and negligible absorption (Tables 1*a*, *b*, *c*) as well. Thus, detailed analysis of the theoretical models

Table 2 (*cont.*)

(*c*) Cu $K\alpha$ tube
$\lambda = 1.5418$ Å, $f' = -1.0885$, $f'' = 0.885$, $\mu = 339.4$ cm^{-1}. $A_{min} = 0.06$ (111), $A_{max} = 0.16$ (711); $X_{min} = 8.6$ (711), $X_{max} = 27.1$ (220)

h	k	l	$\sin\theta/\lambda$	$A^*y_{B\&C}$	y present	I_{calc} (counts s^{-1}) B&C	I_{calc} (counts s^{-1}) present	I_{obs} (counts s^{-1})
1	1	1	0.153	0.001	0.004	57.5	37.3	37.6
−1	−1	−1						36.3
2	2	0	0.250	0.001	0.007	49.0	46.0	47.7
−2	−2	0						47.0
3	1	1	0.294	0.002	0.010	29.4	22.8	23.5
−3	−1	−1						19.8
4	0	0	0.354	0.002	0.012	33.6	32.4	31.7
−4	0	0						29.6
3	3	1	0.386	0.003	0.016	21.4	17.3	19.1
−3	−3	−1						18.0
4	2	2	0.434	0.003	0.016	25.5	25.1	25.0
−4	−2	−2						21.3
5	1	1	0.460	0.004	0.021	16.3	14.2	15.1
-5	−1	−1						12.8
3	3	3	0.460	0.004	0.021	16.3	14.2	15.4
−3	−3	−3						12.4
4	4	0	0.501	0.004	0.022	30.0	27.3	27.9
−4	−4	0						26.1
5	3	1	0.524	0.007	0.031	25.1	18.6	21.0
−5	−3	−1						19.4
6	2	0	0.560	0.007	0.031	51.0	38.8	41.2
−6	−2	0						38.3
5	3	3	0.580	0.013	0.041	52.0	28.4	31.9
−5	−3	−3						23.4
4	4	4	0.613	–	0.038	–	69.2	72.1
7	1	1	0.632	0.002	0.049	16.1	64.7	69.0
−7	−1	−1						60.2
I_0 (counts s^{-1} m^{-2}) × 10^{14}						13 (11)‡	2.2 (2)	
R						410‡	0.061	

† Calculated with $n = 12$ reflections. ‡ Calculated with $n = 26$ reflections.

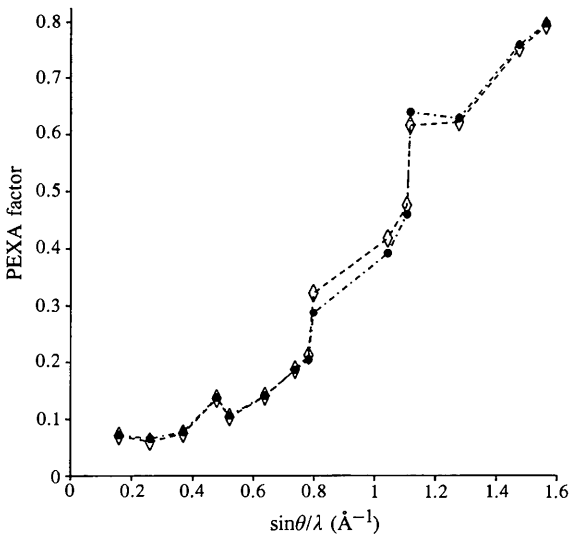

Fig. 1. Primary extinction and absorption correction for Si: case of negligible absorption corresponding to Table 1(*a*). – – – – Line connecting discrete values of $A^*y_{B\&C}$ marked as ◇. – · – · – Line connecting discrete values of y_p marked as ●.

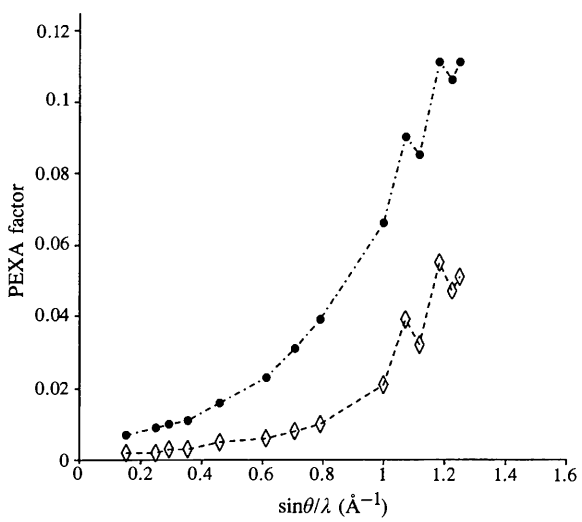

Fig. 2. Primary extinction and absorption correction for Ge: case of high absorption corresponding to Table 2(*a*). – – – – Line connecting discrete values of $A^*y_{B\&C}$ marked as ◇. – · – · – Line connecting discrete values of y_p marked as ●.

and experimental data for silicon and germanium tend to confirm the assertion that, at the desired level of accuracy, there is evidence to choose the present theoretical model for computing PEXA factors, at least in the case of high X-ray absorption.

5. Conclusions

This study demonstrates the importance of the present model to describe both the primary-extinction and absorption properties of X-ray diffraction by finite crystals as the calculated PEXA factors match the experimental data with the desired accuracy. The application of the Laue approximation for the point-source function taking into consideration the X-ray absorption effects provides a quantitative improvement of the fitting to the Bragg intensities that have not been heretofore achieved in this field for absorbing crystals.

Thus, the essential findings of this study are the following:

(i) the 'absorption' modification of the Laue approximation of the point-source function quantitatively describes the combined primary extinction and absorption of the X-rays within finite crystals;

(ii) in contrast with previous theoretical models, the PEXA factor y_p fits the measured Bragg intensities for both Si and Ge spherical crystals at the 3–6% level of accuracy;

(iii) the simple assumption of decomposition of the PEXA factors into the product of the pure extinction and pure absorption factors is not implicit to match the experimental data, at least in the case of strongly absorbing crystals.

References

Al Haddad, M. & Becker, P. J. (1990). *Acta Cryst.* A**46**, 112–123.
Becker, P. (1977). *Acta Cryst.* A**33**, 667–671.
Becker, P. J. & Coppens, P. (1974). *Acta Cryst.* A**30**, 129–147.
Becker, P. J. & Dunstetter, F. (1984). *Acta Cryst.* A**40**, 241–251.
Hamilton, W. C. (1957). *Acta Cryst.* **10**, 629–634.
Kato, N. (1976). *Acta Cryst.* A**32**, 453–457, 458–466.
Laue, M. (1960). *Röntgenstrahlinterferenzen.* Frankfurt am Main: AkademischeVerlagsgesellschaft.
Maslen, E. N. (1992). *International Tables for Crystallography*, Vol. C, edited by A. J. C. Wilson, Section 6.3. Dordrecht/Boston/London: Kluwer Academic Publishers.
Olekhnovich, N. M. & Olekhnovich, A. I. (1978). *Acta Cryst.* A**34**, 321–326.
Rossmanith, E. (1993*a*). *Acta Cryst.* A**49**, 80–91.
Rossmanith, E. (1993*b*). *J. Appl. Cryst.* **26**, 753–755.
Schmidt, H. (1995). Diplomarbeit, Universität Hamburg, Germany.
Takagi, S. (1962). *Acta Cryst.* **15**, 1311–1312.
Takagi, S. (1969). *J. Phys. Soc. Jpn*, **26**, 1239–1253.
Taupin, D. (1964). *Bull. Soc. Fr. Minéral Cristallogr.* **87**, 469–511.
Taupin, D. (1967). *Acta Cryst.* **23**, 25–28.
Werner, S. A. (1974). *J. Appl. Phys.* **45**, 3246–3254.
Werner, S. A., Berliner, R. R. & Arif, M. (1986). *Physica (Utrecht)*, **137**B, 245–255.
Zachariasen, W. H. (1967). *Acta Cryst.* **23**, 558–564.